



Letter

Impact of 1 MeV proton irradiation on InGaAsN solar cells

M Levillayer^{1,2,*} , S Duzellier¹, I Massiot², A Arnoult², S Parola³ , R Rey¹, G Almuneau² and L Artola¹

¹ ONERA/DPHY, University de Toulouse, Toulouse, France

² LAAS-CNRS, Toulouse, France

³ IES, University de Montpellier, CNRS, Montpellier, France

E-mail: maxime.levillayer@gmail.com

Received 11 January 2022, revised 30 March 2022

Accepted for publication 1 April 2022

Published 11 April 2022



Abstract

The impact of 1 MeV proton irradiation on 1.12 eV bandgap InGaAsN solar cells was studied through device and material characterizations. After a $10^{13} \text{ p}^+ \text{ cm}^{-2}$ proton fluence, the photocurrent decreases by 28%, due to the formation of defects in both the GaAs emitter and the InGaAsN absorber. Furthermore, photoluminescence measurements suggest that the proton radiation hardness of InGaAsN increases with the nitrogen.

Keywords: protons, irradiation, InGaAsN, solar cells, PL, EQE, DLTS

(Some figures may appear in colour only in the online journal)

1. Introduction

The current development of artificial satellites requires the conception of powerful and reliable electrical sources that can be used in a space environment. Today, on-board systems rely predominantly on photovoltaic conversion and more specifically on multijunction solar cells (MJSCs).

The MJSCs offer the best conversion efficiencies because they are based on several subcells to harness the solar spectrum, which minimizes transmission and thermalization losses. The most common MJSC used for space applications is the GaInP/(In)GaAs/Ge 3 J cell lattice-matched to its substrate, with 28%–30% efficiency under AM0 sunlight [1]. Research is now being carried out to increase further this efficiency to boost the power density (W kg^{-1}) of space solar arrays. One way of exceeding the 30% efficiency barrier is to optimize the MJSC architecture in order to improve the near

infrared light management. This can be achieved by changing or adding new subcells in the MJSC stack. Indeed, theoretical calculations of the optimal bandgap combination showed that higher efficiencies could be reached by replacing the Ge bottom cell with a 1 eV subcell [2]. Another possibility is to use a 4-junction solar cell by introducing a 1 eV subcell between the GaAs and Ge subcells.

The quaternary alloy InGaAsN is the most promising candidate to be used as a 1 eV absorber in a subcell grown lattice-matched to a Ge or GaAs substrate. Indeed, the bandgap energy and the lattice parameter of this alloy can be tuned with varying the indium and the nitrogen concentration [3, 4].

In addition to lowering the bandgap energy, introducing nitrogen atoms in a GaAs matrix also leads to the creation of crystal defects, which shortens the minority carrier diffusion length [5]. InGaAsN solar cells with a *p-i-n* junction were then developed to take advantage of the drift collection in the space charge region and achieve higher photocurrents [6, 7]. Doing so, high efficiency GaInP/GaAs/InGaAsN 3 J

* Author to whom any correspondence should be addressed.

cells were demonstrated for concentration [8] ($\eta = 43.5\%$, AM1.5D $\times 500$) and space PV [9] ($\eta = 31\%$, AM0).

To be used for space applications, these dilute nitride-based MJSC need to fulfill a crucial requirement: radiation hardness. Indeed, space is a radiative and hostile environment where satellites and other spacecrafts are constantly bombarded by high energy particles such as electrons, protons and heavier ions. Through nuclear elastic interactions with the atoms of the solar cells, these particles generate displacement damage and crystal defects in the lattice. This in turn leads to a decrease in the minority carrier lifetime, which degrades the solar cell properties [10].

Since the subcells in a MJSC are connected in series, the degradation of the photocurrent of a single cell can induce current limitation in the whole structure. Measuring the radiation sensitivity of InGaAsN towards space representative irradiation is then essential to evaluate the end of life (EOL) efficiency of the MJSC. While several studies reported on the effect of electron irradiation on InGaAsN solar cells [9, 11–13], the impact of protons was only investigated for lattice-mismatched dilute nitrides with very low nitrogen content ($<0.5\%$) [14, 15]. In order to fill this lack in the literature and quantify the radiation hardness of InGaAsN towards proton irradiation, we propose a study combining device characterization (I - V and external quantum efficiency (EQE) measurements) with material characterization (photoluminescence (PL) and deep-level transient spectroscopy (DLTS) measurements).

2. Experimental method

InGaAsN solar cells were grown with molecular beam epitaxy on a n -GaAs substrate. The p - i - n solar cell structure consists in a $1\ \mu\text{m}$ -thick non-intentionally doped (NID) InGaAsN absorber sandwiched between 200 nm-thick p - and n -doped GaAs layers. The InGaAsN alloy was grown at $465\ ^\circ\text{C}$ under a As/III flux ratio of 12. The EQE and PL measurements performed on these solar cells indicate a bandgap of 1.12 eV, which corresponds to a 1.6% and a 4.5% nitrogen and indium contents, respectively.

Afterwards, the epitaxial stack was processed into $1\ \text{cm}^2$ devices with a AuGeNi/Au metallization at the rear and a Ti/Au front metal grid. The solar cells were then pasted onto AlN sample holders to facilitate handling during the irradiation and characterization steps. More information regarding the epitaxial procedure and the technological process can be found in [16].

In this study, four InGaAsN solar cells were irradiated under vacuum with 1 MeV protons using a Van de Graaff accelerator [17]. 900 nm-thick InGaAsN bulk layers were also irradiated for PL and DLTS measurements. The samples were cumulatively irradiated at 3.10^{11} , 10^{12} , 3.10^{12} and $10^{13}\ \text{p}^+\text{cm}^{-2}$ fluences with *in-situ* I - V measurements (under both dark and AM0) between each step. The samples were thermoregulated at $26\ ^\circ\text{C}$ during the irradiation steps.

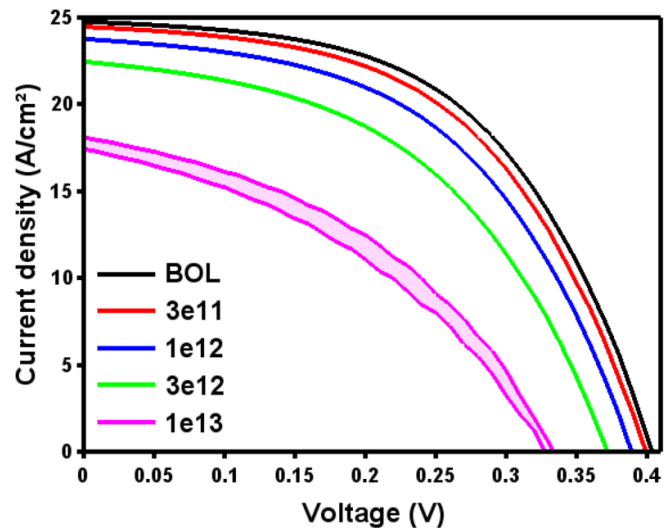


Figure 1. Light J - V characteristics of the InGaAsN solar cells for various fluences (in p^+cm^{-2}) obtained under AM0. The colored area between the two $1 \times 10^{13}\ \text{p}^+\text{cm}^{-2}$ fluence curves represent the dispersion in the J - V degradation within the four cells.

3. Results and discussion

The current–voltage characteristics of the four solar cells were measured *in-situ* at beginning of life (BOL) and after each irradiation step. The solar cells exhibited virtually identical J - V characteristics at BOL. Figure 1 presents the average light J - V characteristics of the cells obtained under AM0 illumination at different fluences. Two J - V curves corresponding to the lowest and the highest degradation are plotted for the final fluence $10^{13}\ \text{p}^+\text{cm}^{-2}$. The small dispersion exhibited here arises likely from a moderate proton flux inhomogeneity and from measurement uncertainties.

Under 1 MeV proton irradiation, the photovoltaic parameters (J_{sc} , V_{oc} and FF) are all degraded. The J_{sc} decrease results from the degradation of the collection efficiency caused by the creation of crystal defects reducing the minority carrier lifetime. The V_{oc} reduction arises both from the photocurrent decrease and from the increase in the dark saturation current density shown in figure 2. This latter parameter increased from $6.6 \times 10^{-7}\ \text{A cm}^{-2}$ to $9.5 \times 10^{-6}\ \text{A cm}^{-2}$ after irradiation.

The average degradation of the J_{sc} , V_{oc} and FF after $10^{13}\ \text{p}^+\text{cm}^{-2}$, is equal to 28%, 18% and 14%, respectively. Although these degradations are quite significant, they remain much lower than the degradation rates exhibited by GaAs solar cells irradiated with 1 MeV protons [18, 19].

We investigated the effect of post-irradiation annealing by exposing the InGaAsN solar cells to AM0 sunlight for 60 min, under thermoregulation. The dark and light J - V characteristics did not show any change after this annealing step, which highlights the stability of the defects introduced throughout proton irradiation.

One of the limitations of the light J - V characterization performed here is that it does not give specific information regarding the degradation of the InGaAsN layer. Under AM0, the

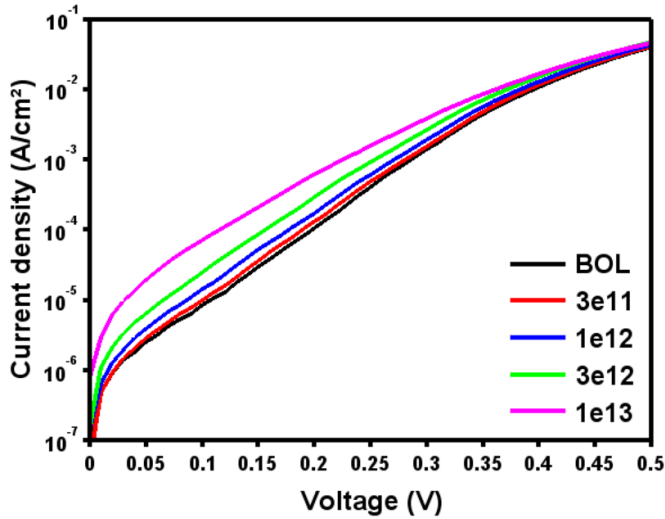


Figure 2. Dark J - V characteristics of the InGaAsN solar cells for various fluences (in p^+cm^{-2}).

carrier collection in the p - i - n subcell arises both from the diffusion in the p -GaAs emitter and from the drift/diffusion regime in the NID-InGaAsN absorber. The global degradation of the cell arises then from the introduction of defects in both InGaAsN and GaAs materials. Yet, only the deterioration of the dilute nitride absorber would be detrimental to a p - i - n subcell integrated within a MJSC structure, as photons with a wavelength shorter than 870 nm would be absorbed in the GaAs middle cell.

As presented in figure 3, EQE measurements were performed on the irradiated solar cells in order to discriminate the degradations of the InGaAsN and GaAs compounds. The quantum efficiency of the InGaAsN subcells shows an overall deterioration, consistent with the photocurrent drop observed in figure 1 and with the dark current increase shown in figure 2. However, the EQE decrease is more important in the (400–870 nm) spectral window, which indicates that part of the J - V degradation arises from the introduction of defects in the GaAs emitter. Using the Beer–Lambert relation and the absorption coefficient of GaAs [20], we calculate that approximately 40% of the 700 nm-photons are absorbed in the 200 nm emitter. The inhomogeneity in the EQE degradation goes in line with the lower radiation hardness of GaAs compared to InGaAsN, as mentioned earlier.

To further investigate the degradation of InGaAsN under proton irradiation, we performed PL measurements on NID-InGaAsN bulk layers of different nitrogen content (1.2% and 2.3%). These samples were excited with a 15 mW 488 nm laser source at room temperature. The PL intensity of the InGaAsN layers is an insightful parameter because it indicates the magnitude of non-radiative recombination and therefore highlights the introduction of defects throughout irradiation.

As represented in figure 4, the PL signal shows a 30% decrease after irradiation in the 1.2% nitrogen layer whereas the other sample remains virtually unaffected by the 1 MeV protons. This radiation hardness discrepancy arises from

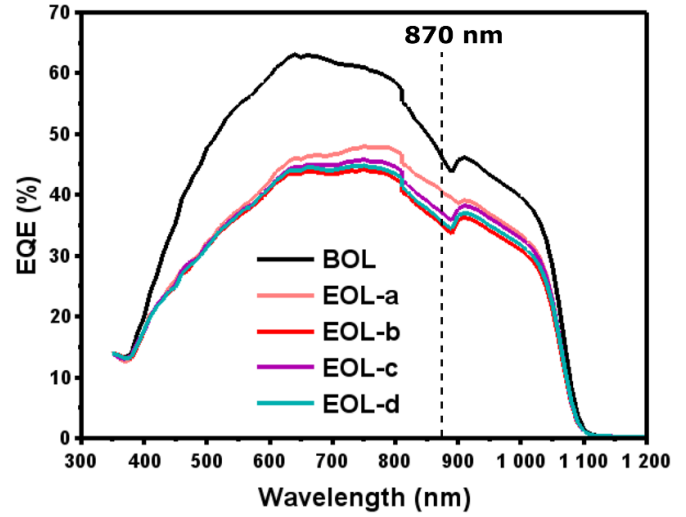


Figure 3. EQE spectra of a non-irradiated InGaAsN solar cell (BOL) and of the four irradiated samples (EOL).

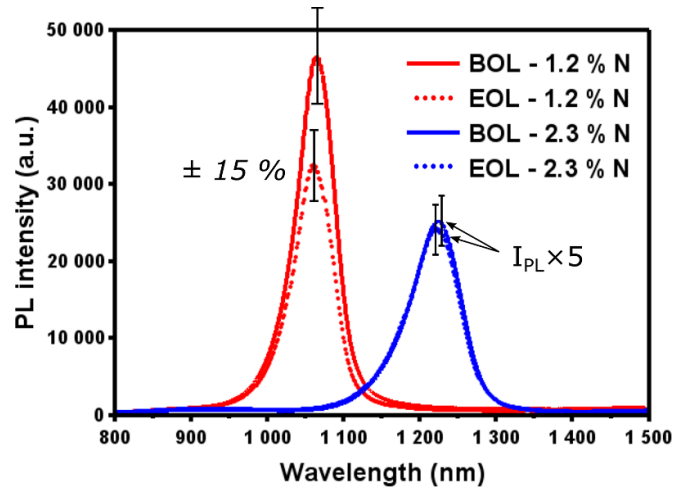


Figure 4. PL spectra of reference (BOL) and irradiated (EOL) InGaAsN bulk layers. The 15% error bars correspond to the measurement uncertainty. The PL intensity of the 2.3% N sample was multiplied by 5 for the sake of clarity.

the difference in the BOL optoelectronic properties of the samples, which can be observed by a PL signal tenfold lower in the 2.3% nitrogen sample. Indeed, the crystal defect concentration tends to increase with the nitrogen content in InGaAsN [21]. In the high N content sample, the irradiation-induced defects concentration is then negligible compared to the density of growth defects. Overall, the PL reduction in the InGaAsN_{0.012} bulk layer sample concurs with the J - V and EQE degradations of the InGaAsN_{0.016} solar cells.

Current-based DLTS measurements were conducted on reference and irradiated bulk layers to investigate the introduction of defects throughout irradiation. We used a current-based rather than a capacitance DLTS mode to avoid parasitic capacitances present in the devices. The residual doping of the NID

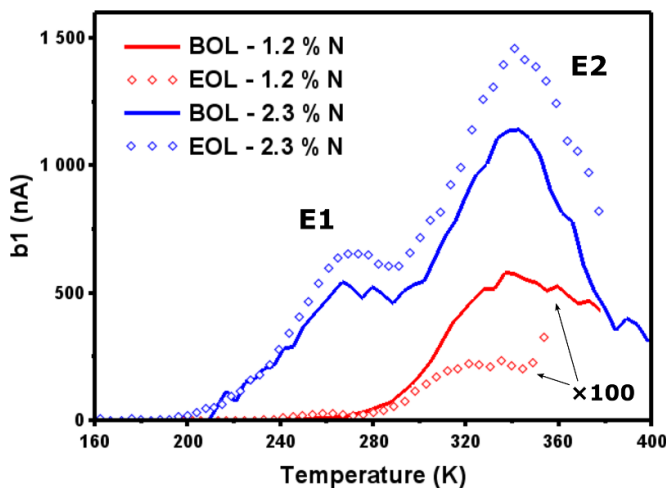


Figure 5. DLTS spectra of reference (BOL) and irradiated (EOL) InGaAsN bulk layers. The DLTS signal intensity of the 1.2% N sample was multiplied by 100 for the sake of clarity.

samples is n-type, meaning that the majority carriers probed here are electrons. The reverse voltage was set to -3 V and we used a 1 ms filling pulse of 1 V. All measurements were performed in the dark condition.

The impact of 1 MeV protons on the DLTS response can be observed in figure 5. It can first be noticed that the DLTS signal $b1$ (first sine term of the Fourier transform) of the high nitrogen content sample increases after irradiation. This signal can be deconvoluted into two peaks at 265 and 340 K corresponding to two electron traps E1 and E2. This increase in the DLTS signal indicates then defect introduction which is in line with our previous observations.

Additionally, the activation energy and the cross-section capture were calculated to be 0.43 eV and $2.7 \times 10^{-16} \text{ cm}^2$ for E1, and 0.63 eV and $4.2 \times 10^{-15} \text{ cm}^2$ for E2. Those two traps lie in the middle of the InGaAsN bandgap and are likely to act as strong non-radiative recombination centers.

The E2 defect is conjectured to be a nitrogen split interstitial as its activation energy was theoretically calculated to be 0.66 eV below the conduction band [22].

On the other side, the DLTS response of the 1.2% content sample is found to drop after the irradiation. This is inconsistent with our PL findings and probably arises from the nature of the irradiation-induced defects. These latter ones are likely to act as hole traps rather than electron traps, making them invisible to DLTS characterization.

4. Conclusion

InGaAsN solar cells and InGaAsN bulk layers were irradiated with 1 MeV protons. The dark and light J - V characteristics of the cells show a monotonic degradation with the proton fluence. The heterogeneous EQE decrease after irradiation indicates that the deterioration of the photovoltaic properties is caused by the introduction of crystal defects in both the GaAs emitter and the InGaAsN absorber.

Moreover, the InGaAsN solar cells studied here are found to be more resistant towards 1 MeV protons than their GaAs counterpart. It can be explained by their higher growth defect concentration, making them less sensitive to irradiation induced defects. This behavior is also supported by the difference in PL degradation exhibited by InGaAsN samples with different nitrogen content. Finally, DLTS results suggest that some of the defects introduced by 1 MeV protons acts as hole traps.

Data availability statement

The data that support the findings of this study are available upon reasonable request from the authors.

Acknowledgments

We acknowledge the technical support from the LAAS-CNRS micro and nanotechnologies platform, a member of the French RENATECH network and the CNES for its support through R-S19/MT-9999-245 project. We also acknowledge the technical support from ONERA for its radiation facilities and characterization platform AXEL. This work was also partly supported by the LAAS-CNRS PROOF platform funded by the Occitanie Region and by the program « Investments for the future » managed by the National Agency for Research under contracts ANR-10-LABX-22-01-SOLSTICE. The authors have no conflict of interest to declare.

ORCID iDs

M Levillayer  <https://orcid.org/0000-0001-6630-470X>
S Parola  <https://orcid.org/0000-0002-2991-3781>

References

- [1] Bett A W, Philipps S P, Essig S, Heckelmann S, Kellenbenz R, Klinger V, Niemeyer M, Lackner D and Dimroth F 2013 *28th European Photovoltaic Solar Energy Conf. and Exhibition*
- [2] Kurtz S R, Myers D and Olson J M 1997 *26th IEEE Photovoltaic Specialists Conf.*
- [3] Kondow M, Uomi K, Niwa A, Kitatani T, Watahiki S and Yazawa Y 1996 *Jpn. J. Appl. Phys.* **35** 1273
- [4] Friedman D J, Geisz J F, Kurtz S R and Olson J M 1998 *J. Cryst. Growth* **195** 409–15
- [5] Kurtz S R, Allerman A A, Seager C H, Sieg R M and Jones E D 2000 *Appl. Phys. Lett.* **77** 400–2
- [6] Jackrel D B, Bank S R, Yuen H B, Wistey M A, Harris J S Jr, Ptak A J, Johnston S W, Friedman D J and Kurtz S R 2007 *J. Appl. Phys.* **101** 114916
- [7] Polojärvi V, Aho A, Tukiainen A, Raappana M, Aho T, Schramm A and Guina M 2016 *Sol. Energy Mater. Sol. Cells* **149** 213–20
- [8] Derkacs D, Jones-Albertus R, Suarez F and Fidaner O 2012 *J. Photon. Energy* **2** 021805
- [9] Campesato R, Tukiainen A, Aho A, Gori G, Isoaho R, Greco E and Guina M 2017 *Proc. 11th European Space Power Conf.*
- [10] Yamaguchi M 1995 *J. Appl. Phys.* **78** 1476–80

- [11] Kurtz S, King R R, Edmondson K M, Friedman D J and Karam N H 2002 *29th IEEE Photovoltaic Specialists Conf.*
- [12] Khan A, Gou J, Kurtz S R, Johnston S W, Imazumi M and Yamaguchi M 2006 *IEEE 4th World Conf. on Photovoltaic Energy Conf.*
- [13] Levillayer M *et al* 2021 *IEEE Trans. Nucl. Sci.* **68** 1694–700
- [14] Bouzazi B, Kojima N, Ohshita Y and Yamaguchi M 2013 *Curr. Appl. Phys.* **13** 1269–74
- [15] Lei Q Q, Aierken A, Sailai M, Heini M, Shen X B, Zhao X F, Hao R T, Mo J H, Zhuang Y and Guo Q 2019 *Opt. Mater.* **97** 109375
- [16] Levillayer M *et al* 2021 *IEEE J. Photovolt.* **11** 1271–7
- [17] Duzellier S, Artola L, Hubert G, Inguibert C, Nuns T, Lewandowski S, Paulmier T, Dirassen B, Rey R and Pons C 2017 *17th European Conf. on Radiation and Its Effects on Components and Systems*
- [18] Pellegrino C, Gagliardi A and Zimmermann C G 2019 *Prog. Photovolt., Res. Appl.* **27** 379–90
- [19] Park S, Bourgoin J C, Sim H, Baur C, Khorenko V, Cavani O, Bourcois J, Picard S and Boizot B 2018 *Prog. Photovolt., Res. Appl.* **26** 778–88
- [20] Palik E D 1998 *Handbook of Optical Constants of Solids* vol 2 (New York: Academic)
- [21] Kurtz S, Johnston S W, Geisz J F, Friedman D J and Ptak A J 2005 *Conf. Record of the Thirty-first IEEE Photovoltaic Specialists Conf.*
- [22] Zhang S B and Wei S H 2001 *Phys. Rev. Lett.* **86** 1789–92